Beyond Limitations of 5G with RIS: Field Trial in a Commercial Network, Recent Advances, and Future Directions

Hyunjun Yang, *Member*, *IEEE*, Sunghyun Kim, Hogyeom Kim, *Member*, *IEEE*, Seungwoo Bang, *Member*, *IEEE*, Yongwan Kim, *Member*, *IEEE*, Seongkwan Kim, Kyujin Park, Doyle Kwon, Jungsuek Oh, *Senior Member*, *IEEE*

***Abstract*—Reconfigurable intelligent surface (RIS) attracts considerable attention as a promising solution to enhance coverage and energy efficiency in 5G communication. In this paper, we validate the performance of RIS in a 5G commercial FR2 band network, proving that it can overcome the coverage limitations of 5G. We first introduce the appropriate hardware design of RIS in mm-wave and explain its performance, including a massive structure, a wide beam coverage, and its ability to transmit wide-band signals without distortion. Then, we describe the topology for field trial construction using RIS-assisted ray-tracing to increase the coverage enhancement performance of RIS in indoor scenarios where coverage prediction is challenging. Finally, we confirm the improvement in indoor coverage and capacity in a commercial network, as demonstrated by an increase in throughput of up to 227.69 percent. To the best of our knowledge, our survey represents the first indoor testbed that evaluates throughput, as well as reference signal received power (RSRP) and signal-to-interference plus noise ratio (SINR) within a commercial FR2 band network. We conclude with some future challenges and the corresponding future research directions.**

***Index Terms*—Reconfigurable Intelligent Surface (RIS), Massive RIS, Field Trial, Commercial Network, 5G Frequency Range 2 (FR2), Liquid Crystal (LC), Unit Cell (UC), RIS-assisted Ray-Tracing.**

I. INTRODUCTION

THE fifth generation (5G) communication is the latest generation of wireless communication that promises to offer significantly faster data speeds, lower latency, and more reliable connectivity compared to its predecessors. Along with the need for these capabilities, the target band in 5G communication extends from frequency range 1 (FR1) to frequency range 2 (FR2), which operates beyond 24 GHz. 5G n257 FR2 band (26.5 – 29.5 GHz) is a focusing spectrum in many countries including South Korea and the United States as well as industries; thus, many researchers have conducted studies on radio frequency (RF) hardware and channel characteristics based on both site-specific measurements and ray-tracing simulation [1], [2]. Consequently, it has been recognized that one of the challenging issues in the mmWave band is the limited coverage owing to high penetration and diffraction loss. Its propagation characteristics have not only led to the expectation that 5G deployment will be concentrated in indoor scenarios, but also prompted mobile network operators (MNOs) to create separate solutions for improving indoor coverage that are distinct from outdoor scenarios, including a distributed antenna system (DAS), repeaters, and small cells [1], [3]. However, these research attempts face challenges for MNOs to satisfy low-cost, low-power consumption, and easy-to-deploy requirements. As an alternative, reconfigurable intelligent surfaces (RISs), which can reflect and redirect radio waves in the desired direction by phase-controllable unit cells, are being developed as promising solutions to enhance coverage and cost-effectiveness.

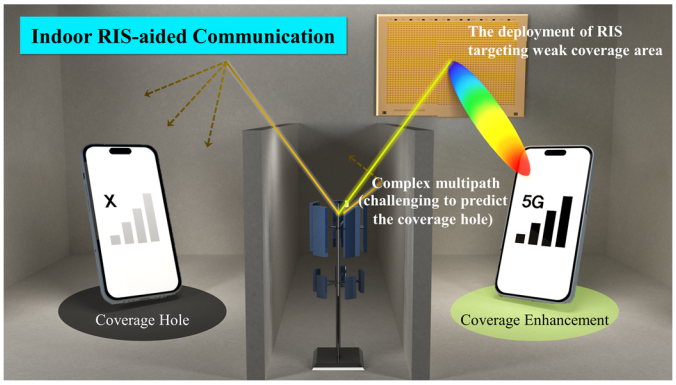

Fig. 1. Indoor RIS-aided communication overview.

Many experimental measurements have demonstrated the capability of RIS. The authors in [4], [5] evaluated the RIS-linked path loss (PL) based on theoretical analyses in free-space, and the authors in [6], [7] conducted measurements in a complex environment where multipath exists. However, experimental realization using a 5G commercial network was barely achieved, and it was not until December 2022 that the first testbed in a 5G commercial network centered at 2.6 GHz

This work was supported in part by KT Corporation (Corresponding author: Jungsuek Oh).

Hyunjun Yang, Hogyeom Kim, Seungwoo Bang, Yongwan Kim and Jungsuek Oh are with the Institute of New Media and Communications (INMC) and the Department of Electrical and Computer Engineering, Seoul National University, Seoul, South Korea (e-mails: guswns6217@snu.ac.kr, ghrua2424@snu.ac.kr, littlebang97@snu.ac.kr, yongwankim@snu.ac.kr, and jungsuek@snu.ac.kr)

Sunghyun Kim, Seongkwan Kim, Kyujin Park and Doyle Kwon are with Infra R&D Center, KT Corp., Seoul, South Korea (e-mails: sh85.kim@kt.com, seongkwan@gmail.com, kyujin.park@kt.com, and doyle.kwon@kt.com)

was published [8]. To the best of our knowledge, indoor testbeds evaluating RSRP, SINR, and throughput in 5G NR band n257 commercial networks, where coverage limitations are more severe than those in the FR1 band, have not yet been presented. Additionally, a massive RIS was designed to compensate for the severe "multiplicative fading" effect introduced by passive RIS, which reflects signals without amplification [5], [9].

The authors in [8] analyzed that the deployment of the RIS contributes more significantly to coverage enhancement in areas with low communication qualities. However, in indoor scenarios, the prediction of the weak coverage areas is challenging due to the rich multipath propagation. Motivated by the aforementioned works, we have focused on RIS-assisted ray-tracing simulation for the deployment topology of RIS as well. Fig. 1 shows a conceptual description of the RIS-deployed scenario for overcoming indoor blind spots.

The main contributions and insights revealed by our survey are as follows.

- **Suitable hardware design of RIS in FR2 band:** Since the RIS-cascaded channel suffers from severe path loss, a massive RIS is designed for receiving the beam without spillover. Furthermore, considering the technical challenges of some active components, we provide the guidelines for the RIS based on liquid crystal (LC), which is the suitable active component in the 5G FR2 band.
- **Guideline for constructing the field trial of RIS in complex propagation channel:** Unlike most existing papers, we measure the RIS coverage enhancement in a more challenging indoor scenario where the base station (BS) and user equipment (UE) are not completely blocked by an obstacle. For this, we utilize our self-developed RIS-assisted ray-tracer, and we present the measurement guideline for effectively evaluating the performance of RIS in realistic environments.
- **The first indoor testbed that evaluates signal quality and network capacity using a commercial FR2 network:** We evaluate the coverage enhancement, including throughput, as well as RSRP and SINR achieved by RIS in a commercial network, and prove the ability to overcome coverage limitations in the 5G FR2 band in the practical scenario mentioned above.

The remainder of this paper is organized as follows. At first, we describe the proposed LC-based RIS. After that, the description for constructing the field trial setup through coverage prediction in the CAD scenario modeling of the indoor office environment is introduced. Subsequently, the results of the first testbed to assess the coverage and network capacity enhancement of RIS using the 5G commercial FR2 band BS are presented. Later on, our conclusions with several future challenges and research directions for RIS are derived in the last section.

II. RIS Hardware operating in FR2 band : Description with tunable components and proposed design

This section introduces the tunable components of RIS, and describes the proposed design for the 5G FR2 band.

A. Recent Works of various tuning elements and Challenges

To realize the RIS, liquid crystal (LC) [10] and semiconductor components, including a positive intrinsic negative (PIN) diode [4], [8] and varactor diode [6], are mainly introduced. In Fig. 2's left, LC is compared with various tuning elements, and the key features are described below.

1) LC: The advantages of LC include cost-effectiveness for massive RIS fabrication, stable frequency response, low power consumption, and continuous RF band phase response. Although it has higher insertion loss than PIN diodes, it exhibits relatively low loss compared to other commonly used tuning elements.

2) PIN diode: PIN diode has the advantage of high cost-effectiveness per diode; thus, many RIS studies have designed RIS based on PIN diode [4], [8]. However, as described in [8], PIN diodes only operate with discrete phase response, which causes significant side lobes and consequently lowers the beamforming gain.

3) Varactor diode: In contrast to PIN diode, varactor diode is capable of providing continuous phase response. However, it has difficulty providing stable frequency responses for wideband owing to its high-quality factors and artificial magnetic conductor characteristics. Moreover, it has the critical disadvantages of exceeding the self-resonance frequency and increasing the energy loss in mm-Wave.

4) Other components: Other semiconductor types include CMOS and HEMT. While CMOS is low-cost in volume production, its high bias complexity increases massive RIS fabrication costs. HEMT has a higher bandgap compared to CMOS, offering advantages in mm-Wave due to its high cutoff frequency, but at the drawback of being high-cost. Also, semiconductor types generate more heat compared to LC. Additionally, there is MEMS, which mechanically adjusts geometry, with low insertion loss as an advantage but durability due to wear as a disadvantage.

B. Proposed Design in FR2 band

In our study, LC was selected as the RIS hardware's reconfigurable material owing to its aforementioned advantages.

1) Design Guideline and Principle: We introduce the proposed LC-based RIS UC, principles for the operating frequency band. As shown in Fig. 2's right, the proposed RIS enables a massive structure consisting of a total of 2250 UCs, and has a size of 0.25 m in width and 0.225 m in height. Such a large-dimensional RIS is designed to overcome the "multiplicative fading" effect, and it can receive a beam without spillover from BS, consequently enabling easy deployment in wireless communication systems. Fig. 2 also shows the proposed LC-based RIS UC in which three TLY-5 dielectrics and four metal layers are used to operate in the desired frequency range. In the LC layer, the cavity for the LC is

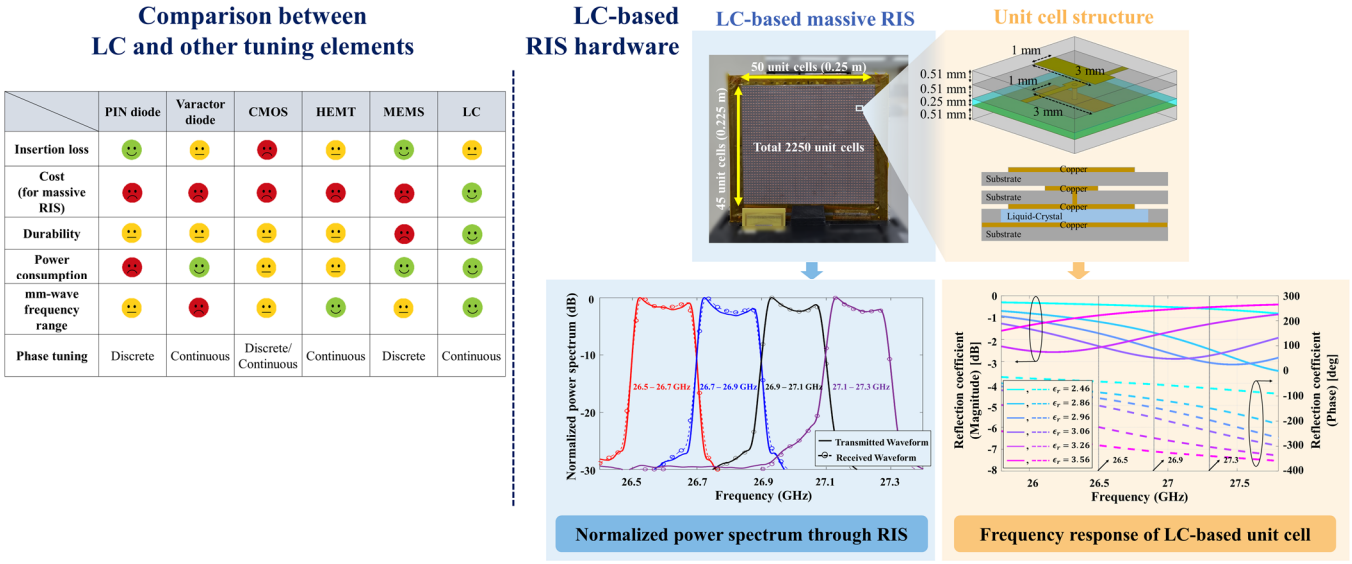

	PIN diode	Varactor diode	CMOS	HEMT	MEMS	LC
Insertion loss	🙂	😐	☹	😐	🙂	😐
Cost (for massive RIS)	☹	☹	☹	☹	☹	🙂
Durability	😐	😐	😐	😐	☹	🙂
Power consumption	☹	🙂	😐	😐	🙂	🙂
mm-wave frequency range	😐	☹	😐	🙂	😐	🙂
Phase tuning	Discrete	Continuous	Discrete/ Continuous	Continuous	Discrete	Continuous

Fig. 2. Comparison of tuning elements and description for the designed and fabricated LC-based RIS hardware. In the figure's right, the simulation result for the magnitude (solid line) and phase (dashed line) frequency responses versus the bias states is presented, and the measured normalized power spectrum of RIS is provided as well.

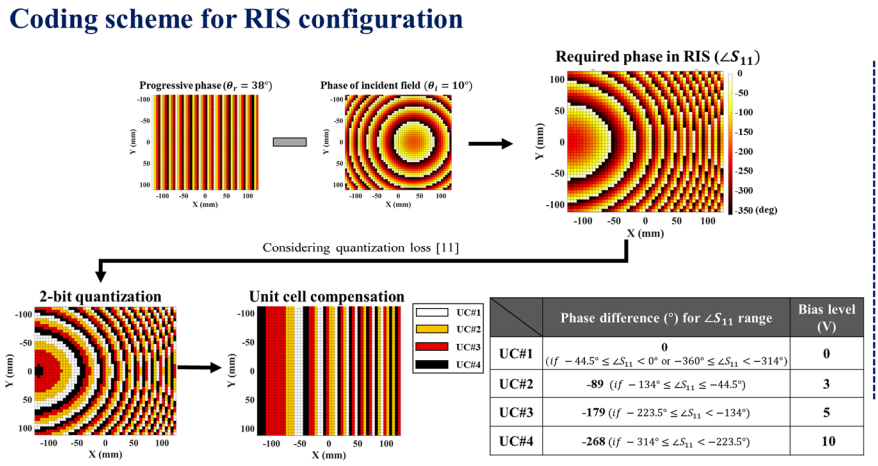

	Phase difference (°) for $\angle S_{11}$ range	Bias level (V)
UC#1	0 ($if\ -44.5° \le \angle S_{11} < 0°$ or $-360° \le \angle S_{11} < -314°$)	0
UC#2	-89 ($if\ -134° \le \angle S_{11} \le -44.5°$)	3
UC#3	-179 ($if\ -223.5° \le \angle S_{11} < -134°$)	5
UC#4	-268 ($if\ -314° \le \angle S_{11} < -223.5°$)	10

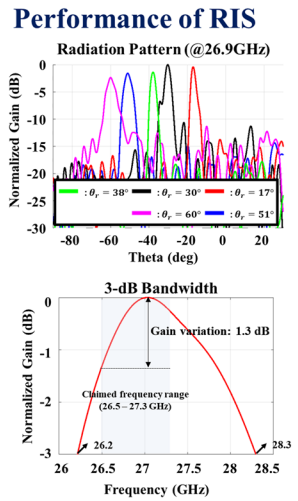

Fig. 3. Coding scheme for RIS configuration, and performance of RIS. For evaluating the beam steering of RIS, the feed horn antenna is set to be 20 cm from RIS. The required continuous phase distribution in RIS, which is $\angle S_{11}$, is calculated by considering the phase of the incident field and progressive phase for beam steering. Considering quantization loss [11], 2-bit quantization of $\angle S_{11}$ range is performed according to the $\angle S_{11}$ range mapping given in the table. Additionally, in the case of 10°-incidence, the measured normalized radiation patterns for various θ_r and 3-dB bandwidth are provided.

supported by the etched TLY-5. A GT7-29001 LC (Merck KGaA, Darmstadt, Germany) was used in this study. Based on the datasheet, the tunable range of the LC dielectric constant used in this study is from 2.46 to 3.56, and the corresponding loss tangent decreases from 0.012 to 0.0064. The dielectric constant and loss tangent of TLY-5 is 2.2 and 0.0009, respectively. The periodicity of the UC was 5 mm. A metal strip was employed to bias the corresponding UCs, and bias signals were applied from the outer control circuit. Novel bias line topologies allow for reliable connections between a control circuitry board and numerous UCs without perturbing RF operations, finally enabling beamforming of the electrical large RIS area. Commercialized BS requires a wide coverage in the azimuthal angle but very narrow coverage in the elevation angle, considering the actual deployment of UE. To address this, the proposed RIS was designed to achieve wide beam coverage along the azimuthal angle from -60 to +60 degrees. Onto the LC layer, the metal patch, connected with metal via, is responsible for exciting the LC layer. A metal layer on the top dielectric was introduced to reduce the reflection loss and enhance the spectral efficiency of the RIS.

2) Performance Description: The simulation results for the frequency response of the proposed UC versus the bias voltage state are shown in the bottom right of Fig. 2. Each color represents the permittivity of the UC with the fixed bias state. Considering the operating commercial FR2 band, the claimed frequency range of the RIS is 26.5 – 27.3 GHz. A required maximum bias voltage of 10 V was confirmed for this bandwidth. With this bias voltage, the power consumption of RIS is 0.045 W. The maximum reflection losses at 26.5, 26.9, and 27.3 GHz are 2.68, 2.83, and 3.05 dB, respectively, and the maximum phase shift range of each frequency point is 248, 268,

and 264 degrees, respectively. Owing to its results, including the low reflection losses and wide tunable phase-shift range provided by the LC, our fabricated RIS can provide a stable frequency response within the target bandwidth. For example, as shown in Fig. 2, the developed RIS can deliver the wide-band signal without waveform distortion. In this figure, signals with a 200 MHz bandwidth at the center frequencies of 26.6, 26.8, 27, and 27.2 GHz are created due to the maximum bandwidth that the signal generator can produce. We compared the normalized waveform received through the RIS and that generated by the signal generator, and the maximum difference between the two waveforms was 0.52 dB, indicating that the distortion of the modulation signal from the 5G commercial BS is not significant in RIS-assisted communication.

Additionally, the coding scheme for configuring RIS and the corresponding performance of RIS, including radiation pattern and bandwidth, are presented in Fig. 3. With this scheme, the RIS beam steering capability is confirmed to cover up to 60 degrees at 10°-incidence. The measured radiation patterns are normalized to the peak of 30°-reflection pattern, and there is a gain reduction of 2.34 dB when the reflection angle is 60 degrees. Additionally, the 3-dB bandwidth is measured to 2.1 GHz, and the peak gain is 30.8 dBi at 27 GHz.

III. Field Trial Construction using RIS-Assisted Ray-Tracing Simulation

This section first introduces the recent advances to consider the re-radiation pattern of an RIS in a ray-tracing system. Then, we present the topology of field trial construction for RIS deployment and performance evaluation in realistic indoor scenarios, unlike most papers which, as in [6] and [8], secured the locations where the BS signal is significantly reduced in advance by considering situations where the BS and UE are fully blocked by an obstacle.

A. Recent Works Related to RIS-Assisted Ray-Tracing

Numerous studies such as [12], [13] have been conducted on how to effectively consider the re-radiation pattern of the RIS in ray-tracing, which many state-of-the-art ray-tracing simulation systems cannot adequately account for. [12] modeled the re-radiation of an RIS using an antenna array based on Huygens's principle. The authors in [13] provided a method to import the RIS into ray-tracing as a secondary transmitter using the radar cross-section (RCS) of the RIS obtained by the finite-element method (FEM). The advantage of obtaining the RCS of the RIS using the full-wave method is that it considers the diffraction at the edge of the RIS and the mutual coupling between UCs. Motivated by the recent progresses, we developed a RIS-assisted ray-tracing simulator applying the [13]'s work. The simulator is built upon SNU 3D Ray-Tracer, which provides high accuracy and fast computation owing to image method and NVIDIA OptiX engine, respectively.

B. Simulation Scenario Setup

As shown in Fig. 4, we conducted CAD modeling of an office environment in the KT Corporation and set the material properties of structures, referring to [14]. In our study, transmission and diffuse scattering were excluded, as well as

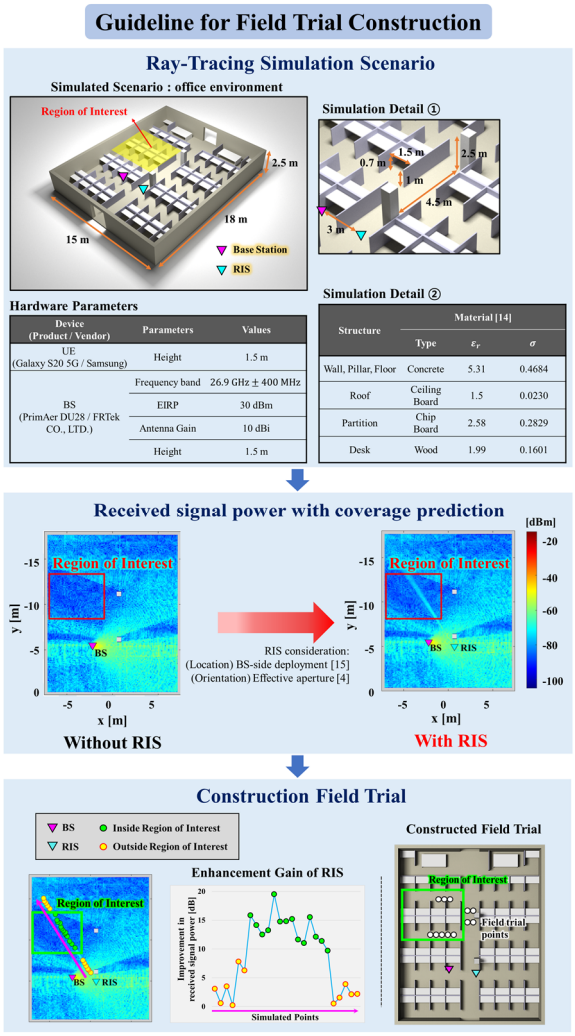

Fig. 4. Topology for the field trial setup that enhances the contribution of an RIS. The simulation shows an improvement in communication quality in the coverage hole. Additionally, it shows that the enhancement gain of an RIS is greater in areas with weak signal than in areas with relatively strong signal.

scatterers such as small plants in the modeling for faster simulation analysis, as described in [2]. Additionally, owing to the limitation of obtaining the exact 3D beam pattern of the UE and BS, we assumed the UE to be an isotropic antenna, whereas the BS was assumed to have a pencil beam expressed as a normalized power radiation pattern in [5] with antenna gain and effective isotropic radiated power (EIRP) in the top of Fig. 4. The heights of the BS, RIS, and UE were set to 1.5 m, which is the height at which people typically hold UE in indoor environments. Furthermore, considering the limited possible areas in which to place the BS during the measurement, we configured the BS beam to be steered across the corridor from the BS location.

C. Coverage Prediction and Field Trial Construction

To predict coverage for both scenarios with and without the RIS, we calculated the incident power at the RIS and the received signal power at the UE, based on the transmit power for the 240 subcarriers located in the synchronization signal block (SSB). Furthermore, the maximum number of reflections

and diffractions was 4 and 1, respectively.

1) without RIS: Through the coverage prediction in Fig. 3, we searched for the area with relatively weak coverage, which is expected to yield a substantial enhancement gain with the implementation of RIS. Consequently, this area was designated as the region of interest where the RIS beams are steered to observe the effect of the main beam.

2) with RIS: For the deployment of RIS and determining the angles of incidence and reflection, we referred to [15] and [4], respectively. According to [15], the BS-side deployment strategy was chosen between the user-side and BS-side, based on the advantages of BS-side deployment including large beamforming gain and large network coverage. Considering the effective aperture of RIS in [4], the surface of the RIS was oriented to closely align with the direction of the BS. Furthermore, the reflection was set at a wide angle within the RIS's scan range, considering the position of the neighboring pillar. Other areas within the region of interest can also be covered through dynamic beam steering. Under the above consideration, we obtained the RCS of the RIS using FEM when the angles of incidence towards the RIS and re-radiation towards the region of interest were 10 and 38 degrees, respectively. Using this RCS pattern as the Tx radiation pattern and the incident power at RIS as the transmit power of Tx, which was calculated as -30.45 dBm according to [13], the RIS-assisted ray-tracing simulation was conducted to calculate wave propagation by the RIS.

As shown in Fig. 4, we confirmed the weak coverage area and the coverage extension to this region. Based on the recent study evaluating coverage enhancement by RIS [8], we constructed the field trial to observe the coverage enhancement by the main beam of RIS within the region of interest. Furthermore, to account for the impact of paths not fully considered in ray-tracing, we also incorporated the surrounding area of the region of interest into the field trial, as shown in Fig. 5.

IV. Field Trial in FR2 band

It should be noted that this field trial is the first testbed that measures RSRP, SINR, and throughput in an indoor environment using the commercial FR2 band BS. Furthermore, this survey will represent a significant milestone for future field trials in many other locations.

A. Recent Work in a 5G Commercial Network

The authors in [8] implemented the field trials to verify the actual performance of coverage enhancement in a 5G commercial FR1 network centered on 2.6 GHz. In [8], they proved that RIS can bring the improvement of communication quality. They emphasized that the contribution of RIS is much more prominent in the coverage hole than in areas with good communication quality. Their research left an important insight into the significance of identifying the coverage hole when conducting field trials in realistic scenarios.

B. Field Trial Scenario

We conducted the measurements in the office, consistent with the scenario described in Section III. In this study, we analyzed key metrics such as RSRP, SINR, and downlink throughput, which are used to assess the signal quality, network capacity, and data rate in a wireless network. A summary of the hardware used in the measurements is presented in the top of Fig. 4. The deployment position of the RIS was selected to closely resemble that used for coverage prediction in Section III. Measurements were conducted at 12 points, including eight points corresponding to Rx 5 to 12 within the region of interest, as shown in Fig. 5. A detailed description of the locations of the BS and RIS is presented in Fig. 5.

Owing to the main lobe beamwidth of the RIS and the complex propagation, it can be expected that coverage improvement for not only the desired direction but also the weak coverage area is possible, as demonstrated in [8].

C. Coverage Enhancement Evaluation

Table I lists the performance verification of the RIS in a 5G commercial FR2 band BS, and the throughput improvement is expressed, considering the small cell characteristic of the indoor systems [3]. At first, we confirmed that the measured RSRP at Rx 5 to 12 were below an average of -100 dBm, verifying their location in a weak coverage area as predicted in Section III. Then, we used two reference cases, corresponding to references 1 and 2, as the baseline values for evaluating the change in network quality. As in [8], reference 1 represents a case without the RIS. Reference 2 corresponds to a case in which the RIS was deployed but turned off, acting as a flat plane and producing specular reflection. We considered the comparison with reference 2 as the accurate result of the throughput improvement. However, this comparison could lead to less throughput improvement than the comparison with reference 1; thus, for the sake of clarity, we have included the results of the comparisons with both references 1 and 2. Furthermore, we collected more than 10 datasets for each Rx position, and used their average values.

Remarkably, a significant network quality improvement in RIS-aided communication was confirmed within the region of interest, where maximum throughput improvements of 227.69 and 184 percent were observed compared to references 1 and 2, respectively. It should be noted that for all Rx points within the region of interest, an improvement in not only the downlink throughput but also RSRP and SINR was confirmed. As an example of the greatest improvement in throughput within the region of interest using reference 2 as the baseline, at Rx 8, RSRP increased from -100.33 dBm to -86.23 dBm, the SINR increased from 8.38 dB to 18.51 dB, and the downlink throughput increased from 0.75 Gbps to 2.13 Gbps.

Additionally, among the remaining 4 Rx points, an average throughput improvement of 65.66 percent was observed at points adjacent to the region of interest, which corresponded to Rx 2 and 4. However, at Rx 1, 12.78 percent decrease in throughput was observed compared to reference 1. As mentioned in [8], this could be attributed to the multipath generated by the RIS causing destructive interference, resulting in a deterioration in communication performance as well as outside the coverage of the main beam from the RIS. Furthermore, instances of lower throughput improvement in

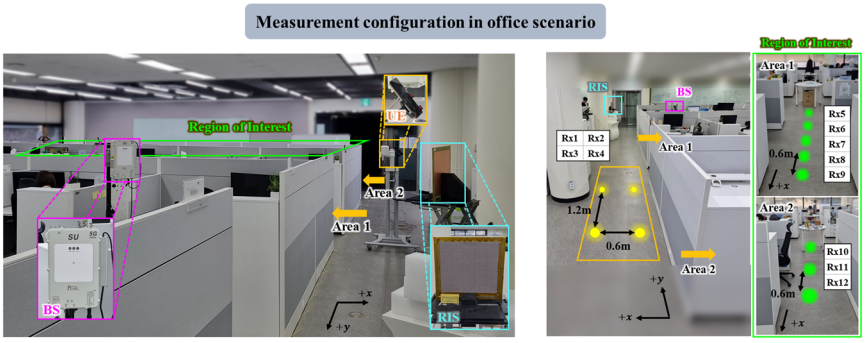

Fig. 5. Measurement overview. Rx 5 to 12 are in the region of interest.

TABLE I
MEASUREMENT RESULTS IN OFFICE SCENARIO

Measurement Sites	Reference 1. Without RIS			Reference 2. With RIS and RIS Off			With RIS and RIS On			Throughput Improvement (%)	
	RSRP [dBm]	SINR [dB]	Throughput [Gbps]	RSRP [dBm]	SINR [dB]	Throughput [Gbps]	RSRP [dBm]	SINR [dB]	Throughput [Gbps]	Baseline, Reference 1	Baseline, Reference 2
Rx 1	-93.43	16.25	1.33	-96.34	14.18	1.18	-93.32	14.77	1.16	-12.78	-1.69
Rx 2	-93.34	13.59	1.19	-93.25	13.54	1.27	-87.71	17.04	2.33	95.80	83.46
Rx 3	-93.42	14.16	1.16	-95.22	13.51	1.14	-95.74	12.23	1.27	9.48	11.4
Rx 4	-97.14	13.27	1.07	-96.17	13.36	1.17	-89.59	17.06	1.73	61.68	47.86
Rx 5	-99.25	12.02	0.96	-96.15	10.15	1	-88.01	18.17	2.38	**147.92**	**138**
Rx 6	-99.66	10.52	0.96	-98.72	13.11	0.94	-87.66	18.29	2.23	**132.29**	**137.23**
Rx 7	-98.29	10.74	0.86	-97.35	13.04	1.11	-80.02	21.52	2.42	**181.4**	**118.02**
Rx 8	-101.25	8.45	0.65	-100.33	8.38	0.75	-86.23	18.51	2.13	**227.69**	**184**
Rx 9	-95.07	14.73	1	-95.08	10.06	1.23	-84.06	21.04	2.36	**136**	**91.87**
Rx 10	-104.07	5.02	0.53	-105.88	4.02	0.44	-99.11	9.58	0.92	**73.58**	**109.09**
Rx 11	-104.22	3.5	0.58	-103.23	7.42	0.53	-95.14	14.57	1.18	**103.45**	**122.64**
Rx 12	-103.13	8.53	0.63	-103.2	5.3	0.68	-90.42	18.96	1.72	**173.02**	**152.94**

* Bold and underlined font indicates points located within the region of interest

baseline 1 than in 2 could also be attributed to multipath variations between the baselines.

In summary, we observed substantial improvements in communication quality at points affected by the RIS's main beam, including those adjacent regions. Specifically, the average gains for RSRP, SINR, and throughput were observed to be 10.14 dB, 7.64 dB, and 1.03 Gbps, respectively, in these areas.

V. FUTURE RESEARCH DIRECTIONS AND CHALLENGES

In this section, we introduce the challenges for RIS and the corresponding future research directions.

A. Design Considerations for RIS

1) Response Time Reduction: In this paper, we presented the LC-based RIS, owing to its advantages, including low power consumption and continuous phase responses at higher frequencies. However, the LC design scheme for achieving fast response time is still an ongoing research topic. Given the demand, [10] significantly reduced response time from several tens of seconds to milliseconds by utilizing dual-frequency LC mixtures, but future research is required for real-time beamforming.

2) STAR-RIS: We considered the employment of reflecting-only RIS, not taking into account the degradation of communication quality caused by RIS blockage for the UE located behind the RIS. Motivated by this viewpoint, the STAR-RIS, which enables full-space coverage by simultaneously reflecting and transmitting, is expected as a new type of RIS.

B. Beam training scheme and Codebook Design for massive RIS

As stated above, coverage enhancement has been proved with massive RIS designed to boost coverage efficiently. However, appropriately reconfiguring the elements of RIS based on channel state information (CSI) in the RIS-assisted system is

likely to provide a higher beamforming gain of RIS. Thus, an efficient method to acquire the CSI is an important future research direction in RIS studies, and one of the considerations is beam training [9]. In contrast to the existing beam training schemes that are designed based on far-field codebooks, massive RIS requires a new codebook design based on the near-field owing to its large aperture size. Accordingly, a low-cost beam training scheme aligned with this new codebook design is proposed as future work.

C. Field Trials for the evaluation of RIS in various scenarios

For the successful establishment of RIS in 5G communication system, RIS should be capable of properly adapting itself in various realistic environments. Thus, future research is required to explore field trials and the RIS-cascaded channel models in complex propagation environments, beyond the ideal scenarios with low multipath. Additionally, while this paper evaluated the coverage enhancement for a single-beam, performance evaluations of other beam-shaping designs, including multi-beam, are likely to be meaningful attempts in scenarios that target multi-users simultaneously.

VI. Conclusion

We first introduced the appropriate hardware design of RIS in mm-wave and explained its performance. Then, we constructed a field trial that enhances the contribution of RIS using RIS-assisted ray-tracer. Finally, we verified the significant coverage enhancement in the 5G commercial FR2 band BS. We concluded with some future challenges and the corresponding future research directions for RIS. To the best of our knowledge, this is the first indoor testbed to verify the performance of an RIS through evaluating RSRP, SINR, and throughput within a commercial FR2 band network. While the successful establishment of RIS requires further research efforts in the future, we believe that our research accomplishments and proposed future directions will contribute to addressing the challenges and providing useful insights in the field of RIS research.

References

[1] S. A. Busari, S. Mumtaz, S. Al-Rubaye, and J. Rodriguez, "5G millimeter-wave mobile broadband: Performance and challenges," *IEEE Communications Magazine*, vol. 56, no. 6, pp. 137–143, 2018.

[2] J.-H. Lee, J.-S. Choi, and S.-C. Kim, "Cell coverage analysis of 28 GHz millimeter wave in urban microcell environment using 3-D ray tracing," *IEEE Transactions on Antennas and Propagation*, vol. 66, no. 3, pp. 1479–1487, 2018.

[3] J. Zhang and G. De la Roche, *Femtocells: technologies and deployment*. John Wiley & Sons, 2011.

[4] J. Jeong, J. H. Oh, S. Y. Lee, Y. Park, and S.-H. Wi, "An improved path-loss model for reconfigurable-intelligent-surface-aided wireless communications and experimental validation," *IEEE Access*, vol. 10, pp. 98 065–98 078, 2022.

[5] W. Tang, X. Chen, M. Z. Chen, J. Y. Dai, Y. Han, M. Di Renzo, S. Jin, Q. Cheng, and T. J. Cui, "Path loss modeling and measurements for reconfigurable intelligent surfaces in the millimeter-wave frequency band," *IEEE Transactions on Communications*, vol. 70, no. 9, pp. 6259–6276, 2022.

[6] A. Araghi, M. Khalily, M. Safaei, A. Bagheri, V. Singh, F. Wang, and R. Tafazolli, "Reconfigurable intelligent surface (RIS) in the sub-6 GHz band: Design, implementation, and real-world demonstration," *IEEE Access*, vol. 10, pp. 2646–2655, 2022.

[7] X. Pei, H. Yin, L. Tan, L. Cao, Z. Li, K. Wang, K. Zhang, and E. Björnson, "RIS-aided wireless communications: Prototyping, adaptive beamforming, and indoor/outdoor field trials," *IEEE Transactions on Communications*, vol. 69, no. 12, pp. 8627–8640, 2021.

[8] J. Sang, Y. Yuan, W. Tang, Y. Li, X. Li, S. Jin, Q. Cheng, and T. J. Cui, "Coverage enhancement by deploying RIS in 5G commercial mobile networks: Field trials," *IEEE Wireless Communications*, 2022.

[9] X. Wei, L. Dai, Y. Zhao, G. Yu, and X. Duan, "Codebook design and beam training for extremely large-scale RIS: Far-field or near-field?," *China Communications*, vol. 19, no. 6, pp. 193–204, 2022.

[10] R. Guirado, P. De la Rosa, G. Perez-Palomino, M. Caño-García, E. Carrasco, and X. Quintana, "Characterization and Application of Dual Frequency Liquid Crystal mixtures in mm-Wave Reflectarray Cells to improve their Temporal Response," *IEEE Transactions on Antennas and Propagation*, 2023.

[11] Q. Wu and R. Zhang, "Beamforming optimization for wireless network aided by intelligent reflecting surface with discrete phase shifts," *IEEE Transactions on Communications*, vol. 68, no. 3, pp. 1838–1851, 2019.

[12] V. Degli-Esposti, E. M. Vitucci, M. Di Renzo, and S. A. Tretyakov, "Reradiation and scattering from a reconfigurable intelligent surface: A general macroscopic model," *IEEE Transactions on Antennas and Propagation*, vol. 70, no. 10, pp. 8691–8706, 2022.

[13] Y. Liu and C. D. Sarris, "Efficient propagation modeling for communication channels with reconfigurable intelligent surfaces," *IEEE Antennas and Wireless Propagation Letters*, vol. 21, no. 10, pp. 2120–2124, 2022.

[14] P. Series, "Effects of building materials and structures on radiowave propagation above about 100 MHz," *Recommendation ITU-R*, pp. 2040–1, 2015.

[15] C. You, B. Zheng, W. Mei, and R. Zhang, "How to deploy intelligent reflecting surfaces in wireless network: BS-side, user-side, or both sides?," *Journal of Communications and Information Networks*, vol. 7, no. 1, pp. 1–10, 2022.

Hyunjun Yang is pursuing an integrated master's and Ph.D. degree at Seoul National University, South Korea.

Sunghyun Kim is a Senior Research Engineer in the Advanced Communications Technology Team at Infra R&D Center, KT Corp.

Hogyeom Kim is pursuing a Ph.D. degree at Seoul National University, South Korea.

Seungwoo Bang is pursuing an integrated master's and Ph.D. degrees at Seoul National University, South Korea.

Yongwan Kim is pursuing a Ph.D. degree at Seoul National University, South Korea.

Seongkwan Kim is the Head of the Advanced Communications Technology Team at Infra R&D Center, KT Corp.

Kyujin Park is a Principal Research Engineer in the Advanced Communications Technology Team at Infra R&D Center, KT Corp.

Doyle Kwon is a Senior Research Engineer in the Advanced Communications Technology Team at Infra R&D Center, KT Corp.

Jungsuek Oh(S'08) is currently an Associate Professor in the Department of Electrical and Computer Engineering, Seoul National University, South Korea.